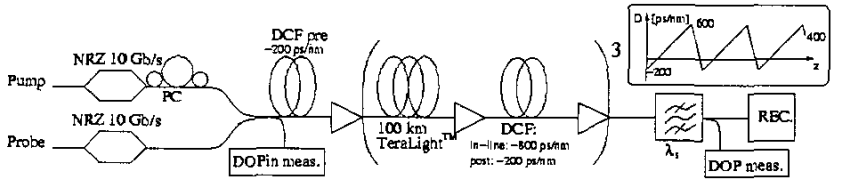

Fig. 1 Experimental set-up for total input DOP(θ) vs output probe DOP measurements. Inset: dispersion map.

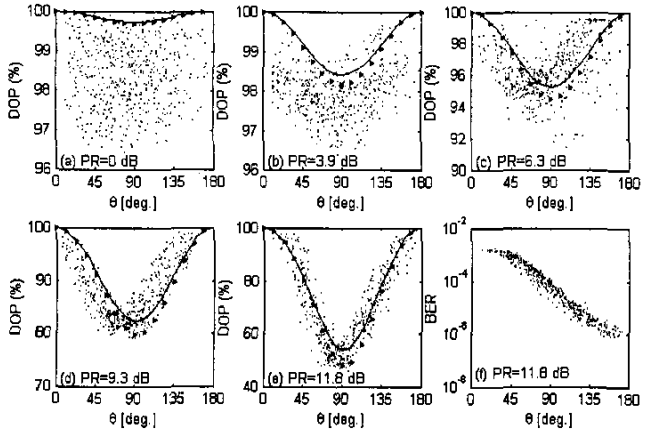

Fig. 2 (a-e)Output probe DOP after 3 spans versus relative input polarization angle θ, for several pump-probe power ratios (PR): measurements (dots), simulations (triangles) and theory (eq. 3) (lines).

Hence, all we need is to evaluate the time-averages in (2).

Now, suppose a string of k consecutive "1" occurs in the pump bit sequence. To evaluate the effect of such string on $\Delta\psi(t)$, we assume to modulate the pump with a periodic sequence of k "1" followed by k "0" and so on. A periodic and skew-symmetric signal $\Delta p(t)$ results with period 2kT, being T the bit period. We can easily evaluate the angle $\Delta\psi(t)$ from (1) if we approximate $\Delta p(t)$ with the first harmonic of its Fourier series expansion: $\Delta p(t) \cong (4/\pi)\sin(\omega_0 t/k)/2$, where $\omega_0=\pi/T$ is the frequency of the 1010... bit sequence. Note that the integral in (1) is the convolution of the normalized pump with a *walk-off filter* $H(\omega)$, whose amplitude response can be approximated as $|H(\omega)|=[\alpha^2+(\omega D_c \Delta\lambda_{sp})^2]^{-1/2}$ for long fibers ($L>>1/\alpha$) [5]. Hence, one gets $\Delta\psi(t)=(8/9)\gamma P_m|H(\omega_0/k)|(4/\pi)\sin(\omega_0 t/k+\varphi_0)/2$. To evaluate the time-averages in (2), we can expand $\cos\Delta\psi(t)$ and $\sin\Delta\psi(t)$ in Fourier series. Averaging over periods much longer than 2kT, one gets $\langle\sin\Delta\psi(t)\rangle=0$, and $\langle\cos\Delta\psi(t)\rangle=J_0(\Delta\psi_M(k))$, where J_0 is the zero-th order Bessel function of the first kind, and $\Delta\psi_M(k)=(8/9)\gamma P_m|H(\omega_0/k)|(4/\pi)/2$ is the maximum swing angle for the probe SOP.

Of course, when the pump is modulated by a pseudo random bit sequence (PRBS), we should consider all possible strings of k ones (k=1... 8). In an uncoded PRBS, the relative occurrence of such strings is $1/2^k$. Resorting to the ergodicity of *the process $\Delta\psi(t)$, we can evaluate the time-average* $\langle\cos\Delta\psi(t)\rangle$ through the summation of $J_0(\Delta\psi_M(k))$ terms weighted by their relative occurrence. Propagation on more than one span can be easily accounted for by multiplying the arguments of the J_0 functions by N_{spans}, provided that fiber losses are recovered and in-line dispersion is perfectly compensated at each span.

The final formula for the DOP is:

$$DOP = \sqrt{1-\sin^2\theta_s\left\{1-\left[\sum_{k=1}^{\infty}\frac{1}{2^k}J_0\left(\frac{(8/9)\gamma P_m (2/\pi) N_{spans}}{\sqrt{\alpha^2+(\pi D_c \Delta\lambda_{sp}/(kT))^2}}\right)\right]^2\right\}} \qquad (3)$$

which is an approximation, since we are only approximating an actual PRBS. The dependence of the DOP on the relative pump-probe polarization angle θ can be made explicit by using the two relations given above for θ_s and P_m. From (3), we see that, if polarization control of the signals ($\theta=180^\circ$ or $\theta=0^\circ$) cannot be achieved, e.g., due to PMD, the basic countermeasure against DOP degradation is to increase the walk-off by further spacing the channels or by using a more dispersive fiber. Increasing the bit rate implies both a smaller T and a larger $\Delta\lambda_{sp}$ in (3), hence a reduction of XPM-induced DOP degradation.

Experimental and simulations results: We performed DOP measurements on the dispersion-managed 3x100 km link depicted in Fig. 1. The dispersion map is shown in the inset. We used TeraLight™ as the transmission fiber, with α=0.2 dB/km, γ=1.68 $W^{-1}km^{-1}$ and D_c= 8 ps/nm/km, whose total measured DGD on the link is below 2 ps, so that PMD can be safely neglected. Pump and probe are spaced by $\Delta\lambda_{sp}$=0.8 nm and are NRZ modulated at 10 Gb/s by independent bit sequences.

We performed five sets of 500 measurements of both the total input DOP and the output DOP, after filtering the probe channel, randomly changing the polarization controller (PC) each time. Fig. 2a-e reports the measured probe DOP (dots) versus θ, along with simulation results (triangles), and the theoretical DOP curve (3) (solid line). The average probe power is fixed at 3 dBm (P_s=6 dBm) while the power ratio PR is varied for each set of measurements. The relative polarization angle θ can be easily calculated from the *measured input DOP and the power ratio PR*.

Fig. 2f reports BER measurements for the same case of Fig. 2e. Without giving details about the receiver, the purpose of this figure is to show that, as θ increases, the efficiency of XPM is reduced by the misalignement of pump and probe polarizations and, as is well known, the best performance is obtained for orthogonally polarized (in Jones space) channels ($\theta=180^\circ$).

All plots in Fig. 2(a-e) have the same V-shape. Their symmetry, however, is related to our system parameters and is not a general feature of (3). In fact, by increasing P_s, a shift of the minimum towards larger θ values is observed from (3). We use different DOP scales to highlight the cases in which the pump power is smaller. The spread in the measurement points is mainly due to the amplifiers noise, which is the main source of depolarization when XPM is negligible (small PR). Such effect is not taken into account in theory and simulations. A very good fit is observed, hence eq. (3) allows an easy closed-form prediction of system behavior with good accuracy.

Conclusions: We derived a closed-form approximate expression for the DOP of a signal degraded by the XPM of a nonlinearly interfering pump. Although in the absence of PMD, DOP degradation does not affect the BER, the quantification of this effect is useful to assess the performance of OPMDCs driven by the DOP as a feedback signal. Experimental measurements, as well as simulations, confirm the good accuracy of the derived expression.

References

[1] E. Corbel, J.-P. Thiéry, S. Lanne, S. Bigo, A. Vannucci and A. Bononi, "Experimental statistical assessment of XPM impact on optical PMD compensator efficiency," *submitted to OFC 2003.*

[2] D. Wang and C. R. Menyuk, "Polarization Evolution Due to the Kerr Nonlinearity and Chromatic Dispersion," *IEEE J. Lightwave Technol.*, **17**, 2520-2529 (1999).

[3] B. C. Collings and L. Boivin, "Nonlinear Polarization Evolution Induced by Cross-Phase Modulation and Its Impact on Transmission Systems," *IEEE Photon. Technol. Lett.* **12**, 1582-1584 (2000).

[4] Z. Pan, Q. Yu, A. E. Willner, and Y. Arieli, "Fast XPM-induced polarization-state fluctuations in WDM systems and their mitigation," in *Proc. OFC 2002, paper ThA7, 379-381 (2002).*

[5] A. Bononi, C. Francia, and G. Bellotti, "Impulse Response of Cross-Phase Modulation Filters in Multi-span Transmission Systems with Dispersion Compensation," *Optical Fiber Technology* 4, 371-383 (1998).

ThJ2 **11:15 AM**

Experimental Statistical Assessment of XPM Impact on Optical PMD Compensator Efficiency

E. Corbel, J. P. Thiéry, S. Lanne, S. Bigo,
Alcatel Research & Innovation, Marcoussis, France; A. Vannucci, A. Bononi,
Università di Parma, Parma, Italy,
Email: Erwan.Corbel@alcatel.fr.

In this paper, we report experiments on the statistical assessment of the reduction of PMD mitigator efficiency in presence of XPM effects. The XPM-induced depolarization limits compensation in polarization dispersive ultra-long haul system at 10 Gb/s.

1. Introduction

Since Polarization-Mode Dispersion (PMD) has been designated as a major impairment for optical transmission systems, many types of optical PMD compensator (OPMDC) have been proposed, starting from the simple mitigator [1] and heading for mitigation of higher-order components of PMD [2].

The system generally corresponds to a non-realistic transmission because it consists of an (higher-order) emulator followed by the compensator. In other words, other propagation effects such as Chromatic Dispersion (CD) and Kerr effects are not often taken into account, for computation time reasons, even if some papers focused on chirp effects on compensation [3] or studied the behavior of Degree of Polarization (DOP) as feedback signal in presence of Self-Phase Modulation (SPM) [4]. That lack is all the more important that we are already aware of the subtle interplay between Kerr non-linearities, chromatic dispersion and PMD [5].

In the same context, some have recently shown that XPM effects make the PMD mitigator be less efficient [6,7]. The purpose of this paper is to experimentally check the reduction of PMD mitigation efficiency from a statistical point of view.

2. Considerations about XPM impact on PMD compensation

In this paper we focus on first-order compensation. It consists of a polarization controller and a piece of Polarization Maintaining Fiber (PMF) (see OPMDC on figure 1-a). The mitigator aims at inverting PMD conditions that the incoming

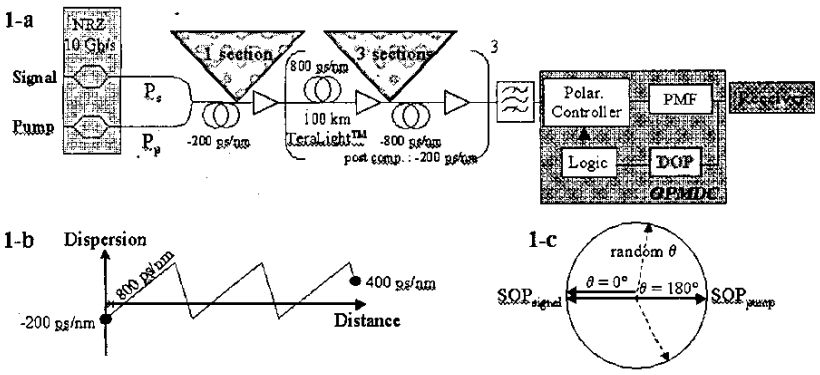

Fig. 1. Experimental set-up with PMD = 30 ps (1-a), dispersion map (1-b) and notations (1-c).

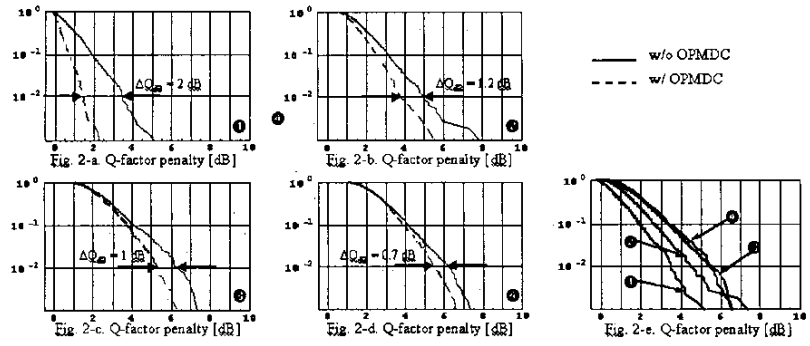

Fig. 2-a. Q-factor penalty [dB]
Fig. 2-b. Q-factor penalty [dB]
Fig. 2-c. Q-factor penalty [dB]
Fig. 2-d. Q-factor penalty [dB]
Fig. 2-e. Q-factor penalty [dB]

Fig. 2. Complement of the cumulative distribution function versus Q-factor penalty with or without PMD mitigation with PMD = 30 ps (❶ linear case; ❷ XPM, θ = 180 °; ❸ XPM, θ = 0°; ❹ XPM, random θ).

signal has undergone during its propagation. Due to stochastic nature of PMD, a feedback loop is required in order to make the inversion adaptive. The feedback signal is chosen to be well correlated with bit-error rate.

B.C. Collings et al. have shown both theoretically and experimentally [8] that XPM effects are responsible for a nonlinear polarization evolution. When considering only two channels at different wavelengths, each state of polarization (SOP) in the Poincaré sphere performs a precession with distance around the mean vector of the two input SOPs. If the channels are amplitude modulated, the SOP of one channel for a given propagation distance will pace to and fro depending whether the other signal propagates a "0" or a "1". This pattern dependence of the state of polarization leads to a depolarization of both channels. A. Vannucci et al. have elaborated a model which describes that depolarization [9]. The latter depends on the conditions of non-linear coupling between the two channels : increasing power or decreasing channel spacing or walk-off make the depolarization more exacerbated. If the relative angle between the two channels equals 0 or 180° in Stokes space, depolarization does not occur. The maximum depolarization appears around 90°. That dependance of SOP with neighbor channels' pattern has two main consequences as far as PMD mitigation is concerned. Firstly, due to the fact that a polarization controller can not move as fast as the current bit-rate (10 Gb/s and higher), the mitigator is unable to follow these variations. Secondly the XPM effects may lead to a distorsion of the dedicated feedback signal : DOP in a straightforward way, as well as spectral lines, eye-monitoring... which are extracted from a distorted electrical spectrum.

In [6], R. Khosravani et al. have numerically studied the reduction of the compensator efficiency with a 8-channel system at 10 Gb/s. In [7], Z. Pan et al. provide an experimental verification of the expected reduction with first-order PMD emulator. In this paper we demonstrate that degradation of PMD mitigator performances in the case of higher-order PMD emulator and from a statistical point of view.

3. System under study

The full set-up is schematically depicted on figure 1. We consider two channels whose spacing is set to 0.8 nm in order to avoid any non-linearly-induced overlap between channels' spectra. Each channel is separately NRZ-modulated with a 10 Gb/s 2^{15}-1 sequence, so as to ensure complete uncorrelation between them. The signal propagates over 3x100 km of TeraLight™ fiber. Because SPM and PMD interplay, the power of signal channel is kept constant and equal to 3 dBm. The power of pump channel can be switched from 3 dBm to 12 dBm, while OSNR of signal channel before filtering remains constant (around 24 dB/0.1 nm). When power of pump is set to 12 dBm, penalty on Q-factor due to XPM effects without PMD is 0.5 dB (resp. 0.8 dB) in the best case i.e. θ = 180° (resp. in the worst case, i.e. θ = 0°) with respect to linear situation (see notations on figure 1-c).

PMD is introduced thanks to a ten-section emulator. Each section consists of a polarization controller and a PMF. The amount of total PMD is 30 ps. Because PMD modifies relative SOPs of two channels with different wavelengths, XPM-induced depolarization is averaged over a part of the range of relative angle between input SOPs ([0…180]). So as to roughly reproduce that mixing over distance, emulation is distributed all along the line. Before the first span of TeraLight™ fiber, we put one section (only first-order PMD) of emulator in order to avoid that relative state of polarization remains the same over the entire first span. Then, 3 sections are added in each inter-stage, before chromatic dispersion compensation fiber (see figure 1).

The feedback loop uses DOP as feedback signal and the DGD brought by compensator is set to 53.1 ps. In presence of PMD, four cases are under study (P_s : average signal power, P_p : average pump power) : **1** linear case with $P_s = P_p$ = 3dBm, **2** non-linear case (XPM) with P_s = 3dBm and P_p = 12 dBm and θ = 180° (cross-polarized channel), **3** non-linear case (XPM) with P_s = 3dBm and P_p = 12 dBm and θ = 0° (co-polarized channel), **4** non-linear case (XPM) with P_s = 3dBm and P_p = 12 dBm and random θ. In the latter case, the relative angle is randomized over the Poincaré sphere, thanks to a programmable polarization controller in the same arm as signal. For each PMD conditions change, a new relative angle between input SOPs is applied, whereas cross-polarization and co-polarization situations are provided thanks to a polarization-maintaining coupler and a polarization-beam coupler. The power on pre-amplifier is set to obtain a BER of 10^{-9} without XPM (pump is switched off) with the constant OSNR (24 dB/0.1 nm) and without PMD.

4. Experimental results

Figure 2-a,d shows experimental results related to the aforementioned cases. It plots the complement of the cumulative distribution function (cdfc) of the Q-factor penalty in decibel with respect to linear transmission. In each case, more than 1000 PMD conditions have been drawn. That is why the cdfc is reliable only down to 10^{-2}.

Without PMD compensation : taking into account intrinsic penalty that stems from XPM effects without PMD, figure 2-e shows that linear PMD-induced penalty can not be simply added to the XPM one, as far as cumulative probability of 10^{-2} is considered. Even if PMD tends to mix the relative angle between channels during propagation, the Q-factor penalty is more relevant when non-linear coupling is most efficient (θ = 0°). The case for which θ is randomized is very close to the worst case. That deleterious interplay between XPM and PMD has already been reported by L. Moller et al. [10].

With PMD compensation : compensation efficiency is assessed by measuring the difference (δQ_{dB}) between Q-factor penalty without and with compensation for a cdfc of 10^{-2}. Figure 2 shows a reduction of PMD compensation efficiency in presence of XPM effects. The cases θ = 0 or 180° suffer from the excursion of relative angle starting from 0 or 180° because of PMD-induced mixing, which leads to XPM-induced depolarization (which adds to PMD-induced one). When the relative angle is randomized, the reduction of PMD compensator efficiency is the most striking because, as expected, a larger XPM-induced depolarization is more likely to occur.

As an extension, the non-linear cross-phase (defined as $\varphi_{NL} = \gamma P_P L_{eff}$ for one span, where L_{eff} is the effective length) which is accumulated after 3x100 km of TeraLight™ with a pump power of 12 dBm equals 1.57 rad. For a more realistic system with equal power 3dBm on each channel, the same amount of cross-phase is reached after a propagation of 2400 km, which corresponds to the range of ultra-long hauls. That is why we consider XPM effects as a major limitation of PMD-compensated long terrestrial links at 10 Gb/s whereas the depolarization is much less deleterious at higher bit-rates, as predicted by model [9].

5. Conclusions

We have experimentally shown, from a statistical point of view, that not only penalty due to PMD is exacerbated in presence of XPM but also XPM-induced depolarization can lead to a degradation of PMD compensator efficiency at 10 Gb/s. This effect should be taken into account when assessing the impact of PMD in ULH transmission systems.

References

[1] F. Roy et al., "A simple dynamic polarization mode dispersion compensator," *in Proc. OFC 99*, TuS4.

[2] J. Poirrier et al., "Optical PMD compensation performance: numerical assessment," *in Proc. OFC 02*, WI3.

[3] S. Lanne et al., "Impact of chirping on polarization-mode dispersion compensated systems," *IEEE Photon. Technol. Lett.*, Vol. 12, No. 11, November 2000, pp. 1492-1494.

[4] N. Kikuchi, "Analysis of signal degree of polarization degradation used as control signal for optical polarization mode dispersion," *J. of Lightwave Technol.*, Vol. 19, No. 4, April 2001, pp. 481-486.

[5] C. R. Menyuk, "Stability of solitons in birefringent fibers. II. Arbitrary amplitudes," *J. Opt. Soc. Am. B*, Vol. 5, No. 2, February 1988, pp. 392-401.

[6] R. Khosravani et al., "Limitations to first-order PMD mitigation compensation in WDM

systems due to XPM-induced PSP changes," *in Proc. OFC 01*, WAA5.
[7] Z. Pan et al., "Fast XPM-induced polarization-state fluctuations in WDM systems and their mitigation," *in Proc. OFC 02*, ThA7.
[8] B.C. Collings and L. Boivin, "Non-linear polarization evolution induced by cross-phase modulation and its impact on transmission system," *IEEE Photon. Technol. Lett.*, Vol. 12, No. 11, November 2000, pp. 1582-1584.
[9] A. Vannucci et al., "A simple formula for the Degree of Polarization degraded by XPM and its experimental validation," *submitted to OFC 03*.
[10] L. Moller et al., "Setup for demonstration of cross channel induced nonlinear PMD in WDM system," *Electron. Lett.*, Vol. 37, No. 5, March 2001, pp. 306-307.

ThJ3 **11:30 AM**

Time Resolved Characterization of the Polarization State of Optical Pulses

O. Buccafusca, P. Hernday,
Agilent Technologies, Santa Rosa, CA,
Email: osvaldo_buccafusca@agilent.com.

A technique to determine the time evolution of the polarization state within an optical pulse is described and example measurements of pulses affected by polarization-mode dispersion are presented.

1. Introduction

The design of high-speed fiber optic telecommunications systems requires careful control of polarization effects in fiber and components. An additional challenge is the interaction of these effects with each other and with other system parameters such as modulation format, chromatic dispersion and fiber nonlinearities. In some cases, such as polarization-mode dispersion (PMD), it may be necessary to actively measure and compensate these effects through the entire link. A broad assortment of analytical and measurement techniques has been developed to characterize polarization effects and design appropriate mitigation techniques [1-7]. In this paper we present a methodology to measure the time evolution of the polarization characteristics, specifically the Stokes parameters, within fast optical pulses. The effectiveness of the technique is demonstrated by measurements of the impact of PMD on narrow pulses. The applications for this type of measurement include pulse/soliton propagation studies, polarization model verification and PMD mitigation research.

2. Measurement Description

The measurement technique involves recording the time-resolved intensity of the pulse after transmission through polarization filters with a known transfer functions [8]. In our setup the filtering functions are provided by the Agilent 8169A polarization controller, which contains a half-wave plate followed by a quarter-wave plate and a polarizer. When the polarizer is set at 0 degrees, the output intensity is given by :

$$I(t)=\frac{S_0(t)}{2}+[\sin^2(2\theta_h-2\theta_q)-\cos^2(2\theta_h)]\frac{S_1(t)}{2}$$
$$+[\sin(4\theta_h-2\theta_q)\cos(2\theta_h)]\frac{S_2(t)}{2}+[\sin(2\theta_q)]\frac{S_3(t)}{2} \quad (1)$$

where θ_q is the angle of $\lambda/4$ plate, θ_h is the angle of $\lambda/2$ plate and S_i is the ith-Stokes parameter. By setting four different independent combinations of angles θ_q and θ_h, the four Stokes parameters can be determined from the following expression:

$$\begin{bmatrix} S_0(t) \\ S_1(t) \\ S_2(t) \\ S_3(t) \end{bmatrix} = \begin{bmatrix} 1 & 1 & 0 & 0 \\ -1 & 1 & 0 & 0 \\ 1 & 1 & -2 & 0 \\ 1 & 1 & 0 & -2 \end{bmatrix} \begin{bmatrix} I_1(t) \\ I_2(t) \\ I_3(t) \\ I_4(t) \end{bmatrix} \quad (2)$$

where $I_1(t)$ is the intensity for the condition $\theta_q = \theta_h = 0$; $I_2(t)$ for the condition $\theta_q = 0$ and $\theta_h = 45°$; $I_3(t)$ for $\theta_q = 0$ and $\theta_h = 22.5°$ and $I_4(t)$ for $\theta_q = 45°$ and $\theta_h = 0$.

By this technique, the measurement of the time-resolved polarization state is reduced to the sequential recording of the intensity traces $I_1(t)$ to $I_4(t)$. The time resolution of the technique is determined by the recording instrument. The use of a photodiode and an electrical sampling scope limits the resolution to about 6-7ps. In this paper, the resolution was improved to about 650fs by using an Agilent 86119A optical sampling oscilloscope. The sequential nature of the measurement method requires temporal stability. Averaging improves the signal to noise ratio, but increases the acquisition time. In the measurements presented in the next section each trace was acquired using averaging times of less than 60 seconds.

3. Results and discussion

We performed measurements on a variety of systems with different pulse sources and fiber types. Due to space constraints, we present only two sets of results involving polarization-maintaining fiber (PMF). This type of fiber has two distinctive principal polarization states (PSP) with different transmission velocities. The differential group delay (DGD) between the PSP's directly broadens the received pulse as the projection in the fast axis accelerates with respect to the slow one. This effect is observed in the first example. A short laser pulse was transmitted through a 2m long piece of polarization-maintaining fiber (PMF). The input pulse was linearly polarized at about 45 degrees relative to a birefringent axis to allow transmission in both fast and slow eigenmodes of the fiber. The pulse duration was measured to be 4ps at the input of the PMF. The time-resolved Stokes parameters, normalized to S_0, are shown in Figure 1, where the time was arbitrarily set to zero at the middle of the pulse. The vertical polarization (zero degree azimuthal angle) was set parallel to the fast birefringent axis. The polarization ellipses at the top of the chart show the state of polarization at each time within the pulse.

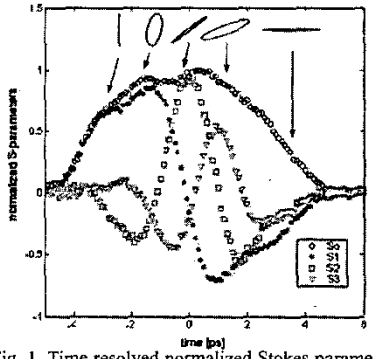

Fig. 1. Time resolved normalized Stokes parameters for the case of a 4ps optical pulse injected in a 2m PMF.

As expected, the pulse was broadened due to the DGD of the PMF. The full-width, half-maximum (FWHM) output pulsewidth of S_0 was measured to be 6.4ps, which is 2.4ps broader than the input. The initial and final polarization states of the output pulse coincide with the linear eigenstates of the PMF. Within the pulse, both the ellipticity and azimuth change significantly. These changes are due to the temporal displacement between the 'fast' and 'slow' components of the optical pulse. This walk-off between the eigenmodes of the PMF affects both the amplitude and phase of the instantaneous electric field within the pulse.

To support the data, we ran a simple simulation that consisted of two gaussian pulses propagating in the eigenstates of the PMF in a quasi-monochromatic approximation. The simulation used a DGD value of 2.7ps, obtained by measuring the actual PMF using the pulse delay method [5]. The simulation was able to reproduce the qualitative evolution of the Stokes parameters, but showed significant deviations around t=0. This was associated to our assumption of gaussian pulses. At t~0, the fast eigenmode intensity is decreasing while the slow one is increasing, consequently the shape of the pulse affects significantly the polarization state. Our assumption of gaussian pulses imposed undesirable limitations because the pulse-shape retrieved from our measurements indicated asymmetric pulse-shapes for the eigenmodes.

The second example also included PMF, but additional components were added to generate elliptical PSP's and produce an arbitrary launching polarization into the PMF. This compound system consisted of a few meters of single-mode fiber, a fiber coil-type polarization adjuster and a 2m long PMF. The length of the fibers was kept short to limit chromatic dispersion. The source in this case was a 1.8ps optical pulse from a fiber ring laser. Because the source pulse was short compared to the DGD of the system, two pulses appeared at the output. Figure 2 shows the time evolution of the S-parameters of the output pulses. The anti-symmetry of S_1, S_2 and S_3 indicates orthogonality, corresponding to the output principal states of polarization of the system. As expected for such a system, the PSP's are not linear.

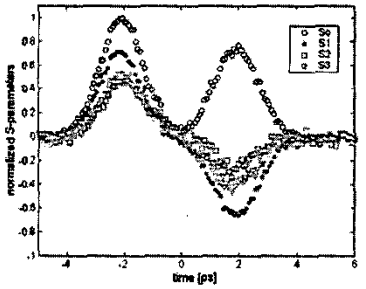

Fig. 2. Time resolved normalized Stokes parameters for the case of a 2ps optical pulse injected in an arbitrary system

Figure 3 shows the Poincaré Sphere plots of the two results just described. The open triangles represent the trace for the first example, 2m of PMF. The points are spaced every 100fs. The initial state is vertically polarized light, according to our system of reference. The final state was in the region of horizontal polarization but exhibited some ellipticity. One possible explanation of this effect is a slight misalignment between the fiber axis and the polarizer, which will be more noticeable for the horizontal polarization. The intermediate states depict a spherical spiral as the amplitude and phase of the pulse changes with time within the pulse. The solid squares in the same figure represent the results in the compound system of the second example, also spaced by 100fs. Two basic clusters are observed, corresponding to the distinct output pulses. These clusters represent the PSP's of our system. The points lie on the surface of the sphere, which indicates a degree of polarization close to unity.

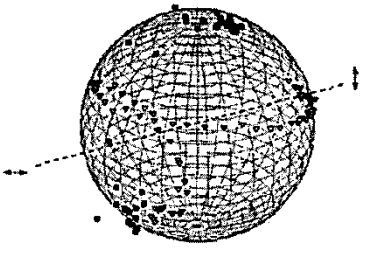

Fig. 3. Evolution of the output polarization state of optical pulses on the Poincaré Sphere. The open triangles represent the case of a 4ps pulse after a 2m long PMF. The solid squares correspond to 1.8ps pulses after a compound fiber system. Points are spaced by 100fs

3. Conclusions

We introduced a technique to measure the time-resolved polarization state of optical pulses. By using an optical sampling scope, we were able to measure the Stokes parameters of short pulses travelling through a PMF. In this case, PMD